

## THE EFFECT OF $\text{CF}_3\text{I}$ COMPARED TO $\text{CF}_3\text{Br}$ ON $\text{OH}\cdot$ AND SOOT CONCENTRATIONS IN CO-FLOWING PROPANE/AIR DIFFUSION FLAMES

KERMIT C. SMYTH AND DAVID A. EVEREST\*

*Building and Fire Research Laboratory  
National Institute of Standards and Technology  
Gaithersburg, MD 20899, USA*

The recent halt in the production of  $\text{CF}_3\text{Br}$  because of its deleterious effect on stratospheric ozone levels has intensified the search for new suppressants with comparable properties. In contrast to most proposed alternatives, earlier investigations of  $\text{CF}_3\text{I}$  have reported excellent extinction efficiencies, sometimes superior to  $\text{CF}_3\text{Br}$  on a molar basis. These findings have spurred an interest in elucidating more clearly the chemical effects produced by iodine-containing suppressants. In the present study,  $\text{OH}\cdot$  and soot concentrations have been measured using fluorescence imaging and laser-induced incandescence methods, respectively, in a co-flowing, axisymmetric, atmospheric-pressure propane/air diffusion flame inhibited by  $\text{CF}_3\text{Br}$  and  $\text{CF}_3\text{I}$ . In addition, broadband molecular fluorescence (attributed to polycyclic aromatic hydrocarbons) has been monitored, and peak temperatures have been measured using two-line  $\text{OH}\cdot$  laser-induced fluorescence. Overall, the two suppressants behave similarly when added to both the air and fuel streams, with the most notable exception being the greater enhancement of soot production for  $\text{CF}_3\text{Br}$  addition at subextinction concentrations.  $\text{CF}_3\text{I}$  is found to be slightly superior to  $\text{CF}_3\text{Br}$  under our experimental conditions in terms of (1) requiring smaller mole fraction concentrations at extinction and (2) producing less within-flame soot. The reductions in the  $\text{OH}\cdot$  concentrations with agent additions are essentially the same for  $\text{CF}_3\text{I}$  and  $\text{CF}_3\text{Br}$ .

### Introduction

For decades,  $\text{CF}_3\text{Br}$  (halon 1301) has been used widely as a suppressant where effective and clean control of fires is needed. However, the bromine atom reacts in a catalytic cycle to destroy ozone in the stratosphere, and as a result of the Montreal Protocol (1987) and subsequent amendments, the production and use of  $\text{CF}_3\text{Br}$  are now greatly restricted. Recent extensive investigations to identify suitable replacements from agents containing only C, H, F, and Cl have not been successful in matching the desirable properties of  $\text{CF}_3\text{Br}$  [1,2]. In contrast,  $\text{CF}_3\text{I}$  has become a leading alternative agent because of its high degree of effectiveness as a flame suppressant coupled with its short tropospheric lifetime and estimated low ozone depletion potential [1-3].  $\text{CF}_3\text{I}$  is the only ready-to-use gaseous agent whose fire-suppression efficacy approaches that of halon 1301, and, thus, for some applications,  $\text{CF}_3\text{I}$  is a virtual drop-in replacement. Concerns remain, however, regarding its use in occupied spaces, discharge and dispersal characteristics at low temperatures (such as in aircraft at high altitudes), and long-term stability and material compatibility [2].

Effective flame suppressants are characterized by

their striking influence on flame propagation chemistry; thus, a clear understanding of how inhibitors influence such processes is valuable in the search for new agents. Prior experimental [1,2,4-7] and modeling [8] studies have found iodine-containing compounds to be comparable to brominated suppressants in terms of concentrations required for extinction and measured decreases in premixed flame speeds. Modeling studies in premixed systems indicate that the Br atom affects the hydrogen atom concentration by catalyzing H-atom recombination into  $\text{H}_2$ , thereby reducing the available radical pool and lowering the overall chain-branching rates [8-10; see also 4,5]. The same mechanism has been invoked for I atoms [8].

The present investigation compares the effects of  $\text{CF}_3\text{Br}$  with those of  $\text{CF}_3\text{I}$  when added to either the air or fuel streams in a steady, co-flowing propane/air diffusion flame. Quantitative  $\text{OH}\cdot$  and soot concentrations are presented.  $\text{OH}\cdot$  has been measured as an indicator of the overall radical pool concentration, although  $\text{H}\cdot$ ,  $\text{O}\cdot$ , and  $\text{OH}\cdot$  are typically not fully equilibrated under diffusion flame conditions [11]. Soot measurements (along with broadband molecular fluorescence) are included because increased soot production has been observed when using suppressants containing bromine (usually evidenced by increased flame luminosity [4,12-17]). However, no quantitative within-flame measurements have been

\*National Research Council NIST Postdoctoral Research Associate, 1994-96.

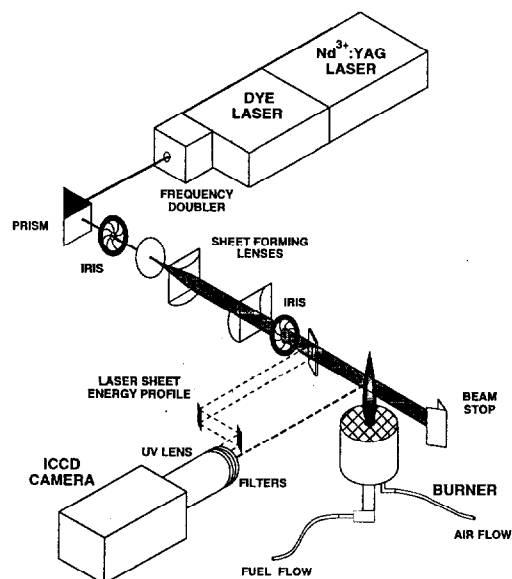


FIG. 1. Experimental setup for one- or two-dimensional imaging of axisymmetric diffusion flames using horizontally polarized UV light. For the laser-induced incandescence experiments, the frequency doubler and sheet-forming optics were removed, and a 300-mm focal length lens was used to focus the visible beam at the center of the flame. Images were recorded using an intensified charge-coupled device (ICCD) camera.

reported, nor has the influence of iodine on soot production been examined previously.

Quantitative radical concentrations and soot volume fraction data are scarce in inhibited flames. In particular, modeling efforts have no experimental database with which to test predictions of iodine-suppression effectiveness in diffusion flames. Comparing how  $\text{CF}_3\text{Br}$  and  $\text{CF}_3\text{I}$  additions affect the key radical  $\text{OH}\cdot$  as well as the local soot concentrations should improve mechanistic understanding, help guide selection of the best delivery strategy for iodine compounds, and aid in the identification of effective flame suppressants.

### Experimental Measurements

Unconfined, axisymmetric, laminar flames were established at atmospheric pressure on a co-annular burner, which consists of a 1.11-cm diameter fuel tube surrounded by a 10.2-cm diameter air annulus. Propane was selected as a typical, moderately sooting hydrocarbon fuel. The cold flow, area-averaged velocity of propane was 2.6 cm/s, and the co-flow air velocity was 10.1–10.6 cm/s. These conditions produced a nonsmoking flame with a visible height (due to soot luminosity) of 85 mm, identical to that stud-

ied recently wherein quantitative soot concentrations and scattering from particles were measured for both steady and flickering flame conditions [18]. Somewhat higher air flows were employed here to minimize HF diffusion to the optics during the agent addition experiments. Furthermore, a 58-cm high shield surrounded the air annulus, with four symmetrically placed 2.5-cm holes for optical access, and full-face gas masks were used during data acquisition.  $\text{CF}_3\text{Br}$  (GL Services,  $\approx 99\%$ ) and  $\text{CF}_3\text{I}$  (Pacific Scientific, 99%) were added to either the air or fuel lines well upstream of the burner to allow for complete mixing, and their flows were monitored using calibrated rotameters.

### OH· Measurements

$\text{OH}\cdot$  imaging measurements were made as in earlier experiments on steady and flickering diffusion flames [18–21]. The  $Q_1(8)$  line of the  $A^2\Sigma^+ \leftarrow X^2\Pi_i(1,0)$  band of  $\text{OH}\cdot$  was excited at 283.55 nm using the frequency-doubled output from a  $\text{Nd}^{3+}:\text{YAG}$  pumped dye laser. This UV beam was formed into a vertical sheet and focused into the flame with cylindrical lenses (see Fig. 1). Laser-induced fluorescence from  $\text{OH}\cdot$  was observed with a Princeton Instruments intensified CCD camera equipped with a Nikon UV lens ( $f/4.5$ , 105 mm) located at  $90^\circ$  to the propagation direction of the laser beam. The pixels were binned by three in each direction, giving an effective spatial resolution of  $258 \mu\text{m}/\text{data point}$  with 3.9:1 imaging optics.

Excitation from the  $N'' = 8$  rotational level minimizes the Boltzmann population correction for temperature variations ( $<5\%$  over the range 1400–2100 K [11]). Low laser energies were used, and checks were made to ensure that the laser-induced fluorescence signals varied linearly with the laser intensity. The intensity profile of the laser sheet was recorded directly on the camera for each laser shot (Fig. 1). A Hoya U-340 filter placed in front of the CCD camera passed light in the range 297–376 nm (50% transmission points) and was used in conjunction with selected long-pass glass filters with nominal cut-on wavelengths near 300 nm to either attenuate or eliminate elastically scattered light from the soot particles while transmitting the (0,0) and (1,1) emission bands of  $\text{OH}\cdot$ .

Since  $\text{CF}_3\text{I}$  strongly absorbs radiation at 283.55 nm [2], measurements were also carried out using excitation of the  $N'' = 8$  rotational line in the (0,0) band at 309.24 nm, where absorption is much reduced. For example, for addition of 1.6%  $\text{CF}_3\text{I}$  to the air stream ( $\sim 45\%$  of the extinction concentration; see later),  $\sim 36\%$  of the 283.55-nm light is absorbed at the location of the peak  $\text{OH}\cdot$  concentration, whereas  $\sim 12\%$  is absorbed at 309.24 nm. The (1,0) band measurements described earlier were corrected for absorption for each concentration of  $\text{CF}_3\text{I}$  added to the air stream.

The absolute  $\text{OH}\cdot$  concentrations can be estimated in the uninhibited propane flame with

reasonable accuracy (within  $\pm 20\%$ ) by comparing fluorescence signals with those obtained in an axisymmetric methane/air flame. For a methane flow velocity of 7.8 cm/s (visible flame height = 79 mm) Puri et al. [19] found that the peak OH $\cdot$  concentration was  $1.59 \times 10^{16}/\text{cm}^3$  for a temperature of 2010 K at a height  $H = 7$  mm above the burner surface. Smyth et al. [11] have observed that (1) H<sub>2</sub>O and CO<sub>2</sub> are the main OH $\cdot$  quenchers at the location of the maximum OH $\cdot$  concentration and (2) the total quenching rate varies slowly over the region where OH $\cdot$  is detected in methane diffusion flames. No detailed species profile data are available for calculating the quenching rates in the propane flames studied here. However, the peak temperatures in the methane and propane flames are almost identical (see later), and the concentrations of CO<sub>2</sub> and H<sub>2</sub>O can be approximated from equilibrium considerations. Because of the lower H/C ratio of propane compared to methane, less H<sub>2</sub>O and more CO<sub>2</sub> are present in the propane flame. The overall effect is an estimated 8% lower quenching rate in the propane flame; that is, an 8% higher fluorescence signal will be observed in the propane flame compared to the methane flame for identical OH $\cdot$  concentrations.

OH $\cdot$  fluorescence signals have been measured in the uninhibited propane flame and in flames with various concentrations of CF<sub>3</sub>Br and CF<sub>3</sub>I added to the air and fuel streams (up to extinction concentrations of  $\sim 4\%$  and  $\sim 45\%$  by volume, respectively). Both inhibitors are likely to decompose at temperatures well below those attained in the primary reaction zone [15,16,22], and their decomposition products may alter the OH $\cdot$  quenching rate and therefore the observed fluorescence signal strength. Saturated (i.e., quenching-independent) OH $\cdot$  fluorescence measurements were made by removing the sheet-forming optics and focusing the entire UV beam ( $\sim 1.1$  mJ/pulse in 5 ns) into the flame with a 300-mm focal length lens. These experiments showed the same trends in OH $\cdot$  levels as in the planar imaging results, but complete saturation was not achieved for the detected signal. Contributions from the spatial and temporal wings of the incident beam arose from the considerable depth of field ( $\pm 1$  mm) of the  $f/4.5$  detection lens and the long detection gate, (19 ns) relative to the pulse duration (5 ns). The overall uncertainty in the OH $\cdot$  concentrations for the inhibited flames due to quenching corrections is estimated to be  $\pm 30\%$ .

### Soot Measurements

Laser-induced incandescence (LII) has been developed recently as a method for making quantitative soot volume fraction measurements [18,21,23–25]. This technique involves the rapid heating of soot particles to temperatures at which their resultant incandescence can be distinguished from both natural

flame luminosity and laser-induced molecular interferences through the use of temporal gating and wavelength filtering. Once the temperature of the irradiated particles reaches the vaporization point (near 4000 K), the LII signal becomes relatively independent of the laser fluence [18,23–25]. LII can provide single laser shot one-dimensional line and two-dimensional planar images with an appropriate high-power laser source and detector array. Validation and calibration of LII as a measure of soot volume fraction is usually based on comparison with soot concentration profiles obtained from reliable extinction measurements (e.g., in well-characterized steady flames).

Laser-induced incandescence of soot particles was excited by focusing the 567-nm dye laser beam with a spherical 300-mm focal length lens. The incandescence signal was recorded as a line image on the intensified CCD camera, using an 85-ns gate that opened coincident with the arrival of the laser pulse. No pixel binning was used on the camera, resulting in a pixel spacing of 86  $\mu\text{m}$ . At low heights, the LII signals showed good reproducibility, so they were collected as 10-shot averages. Starting at  $H = 40$  mm above the burner lip, the LII signals were measured as 10 single-shot frames to allow subsequent minor left-right alignment of the profiles to correct for the effects of flame instability.

A short-pass dielectric 450-nm filter was used for detection of the LII signals. Detection at wavelengths significantly blue shifted from the excitation wavelength of 567 nm eliminates contributions from laser light scattering and also minimizes possible interferences from broadband molecular fluorescence and laser-induced C<sub>2</sub> Swan band emission [18]. Detection at short wavelengths also reduces interferences from natural flame luminosity to insignificant levels.

The laser fluence used for the present LII measurements ( $\sim 5.0$  J/cm<sup>2</sup>) was well above the threshold fluence for which the LII signal variation with laser intensity is small [18,23]. Even with substantial extinction of the beam in the propane flames, the local fluence throughout the soot field was always above the threshold value. Corrections to the raw LII signals were negligible for (1) the fluence dependence of the LII signals due to shot-to-shot variations of the laser intensity and (2) the radial dependence of signal strengths due to the variation of the beam size along the line image [18]. However, extinction of optical signals between their location of origin within the flame and the detector is significant for soot volume fractions  $f_v$  on the order of  $1 \times 10^{-6}$  (1 ppm). Therefore, the laser-induced incandescence signals, once calibrated and averaged about the centerline, were self-corrected for soot extinction, following the analytical procedure of Shadix and Smyth [18]. In the uninhibited propane flame, the maximum LII signal extinction correction

is 15% at  $H = 40$  mm where  $f_{v,max} = 6.3$  ppm and is up to 60% in the inhibited flames where  $f_c$  reaches 29 ppm.

Absolute values of the soot volume fraction in the uninhibited propane flame were obtained from earlier LII measurements [18], which in turn were placed on a quantitative basis by calibration to tomographically inverted HeNe laser extinction measurements of the soot volume fraction in a steady  $\text{CH}_4/\text{air}$  flame [21]. The refractive index selected for converting measured extinctions into local soot volume fractions is  $\bar{m} = 1.57 - 0.56i$ .

### Broadband Fluorescence Signals

Broadband fluorescence from molecular species in fuel-rich flame regions was detected simultaneously with the  $\text{OH}\cdot$  fluorescence in the two-dimensional imaging experiments. This broadband fluorescence has been reported in many earlier studies, including our experiments on Wolfhard-Parker and axisymmetric burners [11,19,26] and has been attributed to polycyclic aromatic hydrocarbons (PAH) [27]. Qualitatively, the intensity of the broadband fluorescence has been found generally to track soot production in diffusion flames and thus has often been associated with soot precursors [28].

### OH· Temperature Measurements

Temperatures were measured from the integrated intensities of two  $\text{OH}\cdot$  rotational lines. The  $P_1(7)$  and  $Q_2(11)$  pair [29] was excited in the  $A^2\Sigma^+ \leftarrow X^2\Pi_i(1,0)$  band of  $\text{OH}\cdot$  by continuously scanning the frequency-doubled wavelength from the dye laser and recording 100 single-shot images. From these, the integrated signal for each line was determined using 15–25 images after background subtraction. Temperature information was thus obtained in the limited spatial region of high  $\text{OH}\cdot$  concentrations, which overlaps the peak temperature location [30]. The results were calibrated against radiation-corrected thermocouple measurements in an axisymmetric  $\text{CH}_4/\text{air}$  diffusion flame using an identical burner [19]. This approach assumes that the added inhibitor affects the quenching and rotational energy transfer rates of the  $P_1(7)$  and  $Q_2(11)$  levels equally.

## Results and Discussion

The focus of our experimental measurements has been on  $\text{CF}_3\text{Br}$  and  $\text{CF}_3\text{I}$  addition to the air stream, since in practical applications these fire suppressants are introduced into diffusion flames from the air side. The base case uninhibited propane flame was operated under nonsmoking conditions with a luminous flame height of 85 mm. Smoke was emitted upon addition of even modest amounts of either sup-

pressant, that is, at levels below 20% of that required for extinction for additions to both the air and fuel streams. At higher agent concentrations, the flames became unsteady and lifted off the burner fuel tube before blow-off extinction occurred. This behavior has been documented previously for  $\text{CF}_3\text{Br}$ -inhibited diffusion flames [31,32].

Extinction occurred for  $\text{CF}_3\text{Br}$  and  $\text{CF}_3\text{I}$  mole fraction concentrations in the air stream of 4.1% and 3.6%, respectively, with an estimated uncertainty of  $\pm 0.3\%$ . Our result for  $\text{CF}_3\text{Br}$  agrees well with values of  $4.3 \pm 0.1\%$  obtained in a co-flow propane/air cup burner diffusion flame [1] and 3.7% in an axisymmetric propane/air diffusion flame [31, Fig. 6]. Much higher concentrations of suppressant are required to extinguish the propane flame for addition of  $\text{CF}_3\text{Br}$  and  $\text{CF}_3\text{I}$  to the fuel stream: 46% and 44%, respectively, in accord with several investigations of bromine-containing [13,31,33–35] and iodine-containing [6] suppressants. This large difference in agent concentrations at extinction in the fuel versus air streams is due mostly to the dilution of the suppressant's concentration in the high-temperature reaction zone when added to the fuel, since stoichiometric burning of 1 mol propane requires 23.8 mol air. A flux analysis supports this simple interpretation [34,35]. In terms of the number of moles of agent required at extinction, Trees et al. [35] found that  $\text{CF}_3\text{Br}$  is  $\sim 2\times$  more efficient when added to the air side in a counterflow  $\text{CH}_4/\text{air}$  diffusion flame. In contrast, for our co-flowing propane flame, a flame sheet analysis indicates that when  $\text{CF}_3\text{I}$  and  $\text{CF}_3\text{Br}$  are added to the air stream,  $\sim 20\%$  more agent is needed at extinction compared to addition to the fuel flow.

### OH· and Broadband Fluorescence Measurements

Figure 2 presents two-dimensional images of  $\text{OH}\cdot$  fluorescence for the uninhibited propane flame as well as for several concentrations of  $\text{CF}_3\text{Br}$  and  $\text{CF}_3\text{I}$  in the air co flow. For both suppressants, the flame first starts to lift off the burner fuel tube for agent concentrations approximately one half of that required for extinction. The images reveal features arising from  $\text{OH}\cdot$  fluorescence in the primary reaction zone (furthest from the centerline) and broadband fluorescence in rich flame regions (closest to the centerline). The  $\text{OH}\cdot$  fluorescence signals exhibit a monotonic decrease with increasing agent concentration. Furthermore, for even the lowest agent concentrations investigated ( $\sim 0.6\%$ ), the flame tip opens and smoke is emitted (evident from soot scattering measurements, not shown in Fig. 2). The broadband fluorescence is strongest at low flame heights and exhibits a dramatic increase for additions of  $\text{CF}_3\text{Br}$  compared to the uninhibited flame, while a smaller increase is evident for  $\text{CF}_3\text{I}$ .

Figure 3 shows selected line profiles extracted

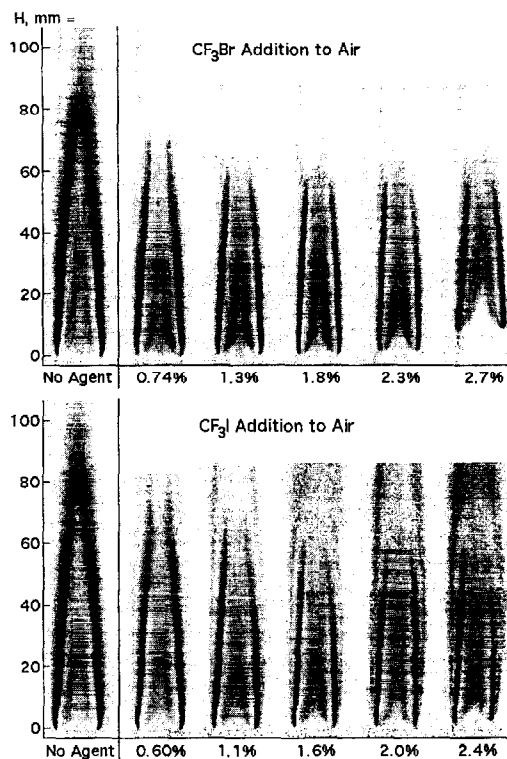


FIG. 2. Laser energy-corrected  $\text{OH}\cdot$  and broadband fluorescence in steady laminar  $\text{C}_3\text{H}_8/\text{air}$  diffusion flames with various levels of  $\text{CF}_3\text{Br}$  (top) and  $\text{CF}_3\text{I}$  (bottom) added to the air stream. For both suppressants, the maximum concentration shown here corresponds to  $\sim 67\%$  of that required for extinction.  $\text{OH}\cdot$  fluorescence in the primary reaction zone occurs furthest from the centerline, and broadband fluorescence in rich flame regions lies closest to the centerline. The visible flame height of the uninhibited flame is 85 mm above the fuel tube exit, which is located at the bottom of the images.  $\text{OH}\cdot$  fluorescence signals have not been corrected for local quenching rates (see text). Four or five 10-shot images (33 mm high) have been overlapped because of reduced signal to noise at the upper and lower edges of the incident laser sheet. Several of the stacked images have been shifted slightly side to side to compensate for flame wobble at higher flame locations.

from the two-dimensional images of Fig. 2 for conditions in which the flames have not lifted off the fuel tube. The reduction in peak  $\text{OH}\cdot$  signals (summarized in Table 1) is essentially the same for both suppressants. The only other quantitative  $\text{OH}\cdot$  measurements for inhibited diffusion flames are those of Masri et al. [17], who also measured a significant decrease for  $\text{CF}_3\text{Br}$  addition to the air side of a methane/air diffusion flame. For agent concentrations of 1.6% and 1.8% ( $\sim 45\%$  of the extinction concentration), the broadband fluorescence increases by

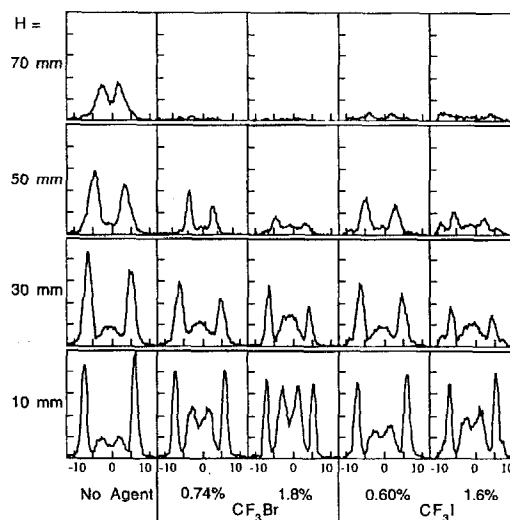


FIG. 3.  $\text{OH}\cdot$  and broadband fluorescence profiles (arbitrary units) at selected heights above the fuel tube from the two-dimensional images presented in Fig. 2, scaled relative to the  $\text{OH}\cdot$  fluorescence signal for the uninhibited propane flame at  $H = 10$  mm. At the bottom of the figure, the agent concentration in the air stream and the radial position (in mm) are indicated. Three rows of data have been summed together at each height. Absorption of the incident laser radiation by  $\text{CF}_3\text{I}$  has been accounted for.

more than three times for  $\text{CF}_3\text{Br}$  at a height of 10 mm above the burner, while a doubling of this fluorescence signal is observed for  $\text{CF}_3\text{I}$  addition. Lerner and Cagliostro [6] also reported an increase in the production of large molecules from absorption measurements in HI-inhibited propane/air flames.

Similar trends were observed for agent addition to the fuel stream, namely (1) tip opening and smoke emission with relatively low agent additions, (2) decreasing  $\text{OH}\cdot$  concentrations with increasing agent concentrations, (3) comparable effects on the  $\text{OH}\cdot$  concentrations for  $\text{CF}_3\text{Br}$  and  $\text{CF}_3\text{I}$ , and (4) enhanced broadband fluorescence that is stronger with the addition of  $\text{CF}_3\text{Br}$  compared to  $\text{CF}_3\text{I}$ . Selected images are presented in Fig. 4. Agent addition to the fuel stream produces flames with a more complex fluorescence structure in the fuel-rich regions than for addition to the air side (compare to Fig. 2).

#### $\text{OH}\cdot$ Temperature Measurements

Table 1 includes peak temperatures determined from the integrated intensities of two  $\text{OH}\cdot$  rotational lines for the uninhibited propane flame, as well as for  $\text{CF}_3\text{Br}$  and  $\text{CF}_3\text{I}$  additions to the air stream at  $\sim 45\%$  of the concentration required for extinction. Measurements are given at low flame heights, where the inhibited flames were sufficiently stable to obtain

TABLE I  
Normalized peak OH· concentrations, soot volume fractions, and maximum temperatures in propane/air diffusion flames with CF<sub>3</sub>Br and CF<sub>3</sub>I added to the air stream

<i>H</i> , mm	Propane No Agent	CF <sub>3</sub> Br			CF <sub>3</sub> I		
		0.74%	1.8%	2.7%	0.60%	1.6%	2.4%
OH· Concentration (Linear fluorescence) <sup>a</sup>							
70	0.40	0.04	0.0	0.0	0.08	0.0	0.0
50	0.67	0.46	0.19	0.28	0.40	0.23	0.19
30	0.99	0.68	0.64	0.56	0.67	0.42	0.54
10	1.0	0.93	0.83	0.75	0.80	0.78	0.73
Soot Volume Fraction <sup>b</sup>							
70	0.60	3.6	7.7	3.2	1.3	4.5	6.1
50	1.2	4.1	5.4	3.3	2.5	4.2	4.9
30	1.0	2.2	2.6	0.97	1.3	1.7	1.5
10	0.030	0.25	0.52	0.0	0.091	0.18	0.069
OH· Two-Line Temperature, K <sup>c</sup>							
40	2025 ± 31		2103 ± 22				
30	2093 ± 50		2019 ± 51				
20	2021 ± 51		2082 ± 39			2029 ± 34	
10	2008 ± 14		1926 ± 25			2048 ± 45	

<sup>a</sup>Maximum OH· concentration is  $1.68 \times 10^{16}/\text{cm}^3$  at  $H = 10$  mm in the uninhibited propane flame (see text). Measurement reproducibility is  $\pm 5$ –13%, and quenching rate uncertainties are  $\pm 30\%$ .

<sup>b</sup>Calibration point is at  $H = 30$  mm in the uninhibited flame, where the maximum soot volume fraction is  $3.8 \times 10^{-6}$ ,  $f_{v,\text{max}}$  in this flame is  $6.3 \times 10^{-6}$  and occurs at  $H = 40$  mm [18]. Measurement reproducibility is  $\pm 5$ –14%.

<sup>c</sup>Calibration is at  $H = 7$  mm in a CH<sub>4</sub>/air flame (see text). Quoted uncertainty is for five points at the location of the maximum temperature after  $3 \times 3$  filtering of the images to determine the mean values.

reliable results. Only small temperature differences are evident. Earlier investigations have yielded mixed results: substantially higher maximum temperatures were found for CF<sub>3</sub>Br-inhibited heptane/air [15] and methane/air [17] diffusion flames compared to the uninhibited cases, but a slightly lower peak temperature has been reported for a CF<sub>3</sub>Br-inhibited counterflow ethylene/air diffusion flame [34].

#### Soot Measurements

An undesirable consequence of using CF<sub>3</sub>Br as a fire suppressant is the large increase in soot production that occurs for agent concentrations below extinction levels. As mentioned previously, several groups have found that bromine-containing inhibitors strongly promote soot formation [4,12–17]. Figure 5 presents the results of calibrated laser-induced incandescence soot measurements for additions of CF<sub>3</sub>Br and CF<sub>3</sub>I to the air stream. Both inhibitors enhance soot production relative to the uninhibited flame, beginning at low heights above the burner and thus early times. For low agent concentrations, CF<sub>3</sub>Br is especially effective as a soot promoter, in parallel with the significantly stronger broadband

fluorescence observed with even small additions of this suppressant (Figs. 2–4). When CF<sub>3</sub>Br and CF<sub>3</sub>I were added at  $\sim 45\%$  of their extinction concentrations (1.8% and 1.6%, respectively), the maximum observed soot concentrations were found to be 4.7 and 2.8 times larger than in the uninhibited propane flame, respectively (Table 1).

Why does CF<sub>3</sub>Br (and to a lesser extent CF<sub>3</sub>I) promote soot formation? Prior investigators have speculated that Br catalyzes fuel pyrolysis via H-atom abstraction reactions [14,16]. However, Garner et al. [4] found that Br substitution for Cl in halogenated methanes increased smoke emission despite the fact that H-atom abstraction by Cl should occur much more readily than by Br (the bond energy of HCl [428 kJ/mol, Ref. 36] is much stronger than that of HBr [363 kJ/mol, Ref. 36]). The HBr bond is also considerably weaker than the weakest C–H bond strength in propane (410 kJ/mol [37]), so one would expect that H-atom abstraction from the parent fuel would be relatively ineffective, even at elevated temperatures. The bond energy of HI is even lower (295 kJ/mol [36]), such that iodine atoms do not participate in H-atom abstraction reactions. CF<sub>3</sub> radical is more likely to promote fuel pyrolysis, since the C–H bond energy in CF<sub>3</sub>H is sufficiently strong (448

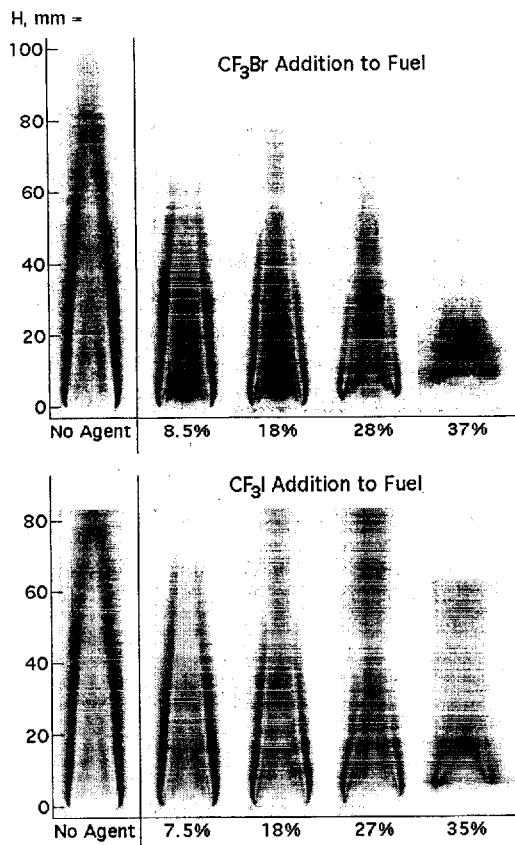


FIG. 4. Laser energy-corrected  $\text{OH}\cdot$  and broadband fluorescence in steady laminar  $\text{C}_3\text{H}_8/\text{air}$  diffusion flames with various levels of  $\text{CF}_3\text{Br}$  (top) and  $\text{CF}_3\text{I}$  (bottom) added to the fuel stream. For both suppressants, the maximum concentration shown here corresponds to  $\sim 80\%$  of that required for extinction.  $\text{OH}\cdot$  fluorescence in the primary reaction zone occurs furthest from the centerline, and broadband fluorescence in rich flame regions lies closest to the centerline. The visible flame height of the uninhibited flame is 85 mm above the fuel tube exit, which is located at the bottom of the images.

$\text{kJ/mol}$  [38]) for  $\text{CF}_3\cdot$  to readily abstract H atoms from propane. It is noteworthy that Br and I act to catalyze H-atom recombination [8], yet H atoms are often invoked as the driving force for soot inception chemistry [39]. Any soot-promoting effects of  $\text{CF}_3\text{Br}$  and  $\text{CF}_3\text{I}$  must overcome the influence of Br and I atoms on reducing the H-atom concentration.

### Conclusions

$\text{CF}_3\text{Br}$  and  $\text{CF}_3\text{I}$  behave similarly when added to both the air and fuel streams of a co-flowing propane/air diffusion flame in terms of significantly re-

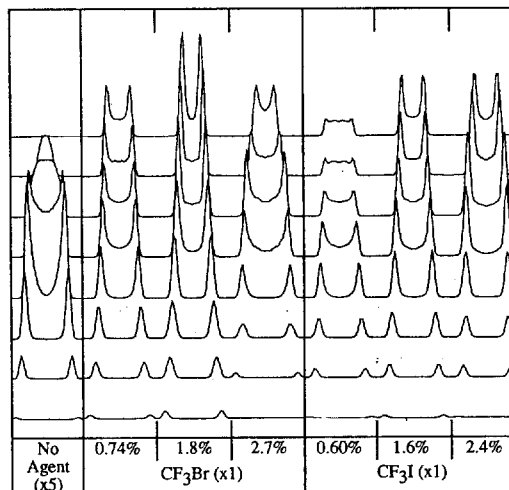


FIG. 5. Profiles of LII-measured soot volume fractions in the uninhibited propane flame compared to those with  $\text{CF}_3\text{Br}$  and  $\text{CF}_3\text{I}$  added to the air stream. Note the indicated relative scalings and that the zero level has been offset at each height; maximum soot volume fraction values are given in Table 1. The profiles extend from  $+5.25$  to  $-5.25$  mm radially for each flame and from  $H = 10$ – $80$  mm above the burner lip, with 10-mm increments in height. All of the profiles have been averaged about the centerline. Note that the flames are lifted for the highest agent concentrations (see Fig. 2).

ducing the  $\text{OH}\cdot$  concentration and, thus, presumably, the H-atom concentration as well. Both agents increase within-flame soot production for subextinction concentrations, with considerably larger effects measured for  $\text{CF}_3\text{Br}$ .  $\text{CF}_3\text{I}$  is also slightly superior to  $\text{CF}_3\text{Br}$  as a suppressant, requiring smaller mole fraction concentrations at extinction. Neither agent produced a measurable change in the peak flame temperature at early times.

### Acknowledgments

We thank Anthony Hamins and Greg Linteris for helpful and stimulating conversations and Bill Grosshandler and Dick Gann for their support of this work.

Certain commercial products and equipment are identified herein to adequately specify the experimental procedure. Such identification does not imply recommendation by the National Institute of Standards and Technology, nor does it imply that this equipment is the best available for the purpose.

### REFERENCES

- Grosshandler, W. L., Gann, R. G., and Pitts, W. M., Eds., "Evaluation of Alternative In-Flight Fire Sup-

- pressants for Full-Scale Testing in Simulated Aircraft Engine Nacelles and Dry Bays," NIST SP 861, 1994.
2. Gann, R. G., Ed., "Fire Suppression System Performance of Alternative Agents in Aircraft Engine and Dry Bay Laboratory Simulations," NIST SP 890, 1995.
  3. Solomon, S., Burkholder, J. B., Ravishankara, A. R., and Garcia, R. R., *J. Geophys. Res.* 99:20929-20935 (1994).
  4. Garner, F. H., Long, R., Graham, A. J., and Badakhshan, A., *Sixth Symposium (International) on Combustion*, Reinhold, New York, 1957, p. 802.
  5. Rosser, W. A., Wise, H., and Miller, J., *Seventh Symposium (International) on Combustion*, Butterworths, London, 1959, p. 175.
  6. Lerner, N. R. and Cagliostro, D. E., *Combust. Flame* 21:315-320 (1973).
  7. Sheinson, R. S., Penner-Hahn, J. E., and Indritz, D., *Fire Safety J.* 15:437-450 (1989).
  8. Westbrook, C. K., *Nineteenth Symposium (International) on Combustion*, The Combustion Institute, Pittsburgh, 1982, p. 127.
  9. Westbrook, C. K., *Combust. Sci. Technol.* 23:191-202 (1980).
  10. Westbrook, C. K., *Combust. Sci. Technol.* 34:201-225 (1983).
  11. Smyth, K. C., Tjossem, P. J. H., Hamins, A., and Miller, J. H., *Combust. Flame* 79:366-380 (1990).
  12. Street, J. C. and Thomas, A., *Fuel* 34:4-36 (1955).
  13. Simmons, R. F. and Wolfhard, H. C., *Trans. Faraday Soc.* 52:53-59 (1956).
  14. Ibricu, M. M. and Gaydon, A. G., *Combust. Flame* 8:51-62 (1964).
  15. Kent, J. H. and Williams, F. A., *Fifteenth Symposium (International) on Combustion*, The Combustion Institute, Pittsburgh, 1975, p. 315.
  16. Seshadri, K. and Williams, F. A., in *ACS Symposium Series 16, Halogenated Fire Suppressants* (Gann, R., Ed.), Washington, DC, 1975, pp. 169-182.
  17. Masri, A. R., Dally, B. B., Barlow, R. S., and Carter, C. D., *Combust. Sci. Technol.* 113-114:17-34 (1996).
  18. Shaddix, C. R. and Smyth, K. C., *Combust. Flame* (1996), accepted.
  19. Puri, R., Moser, M., Santoro, R. J., and Smyth, K. C., *Twenty-Fourth Symposium (International) on Combustion*, The Combustion Institute, Pittsburgh, 1992, p. 1015.
  20. Smyth, K. C., Harrington, J. E., Johnsson, E. L., and Pitts, W. M., *Combust. Flame* 95:229-239 (1993).
  21. Shaddix, C. R., Harrington, J. E., and Smyth, K. C., *Combust. Flame* 99:723-732 (1994) and 100:518 (1995).
  22. Creitz, E. C., *J. Chromatographic Sci.* 10:168-173 (1972).
  23. Quay, B., Lee, T.-W., Ni, T., and Santoro, R. J., *Combust. Flame* 97:384-392 (1994).
  24. Vander Wal, R. L. and Weiland, K. J., *Appl. Phys. B* 59:445-452 (1994).
  25. Bengtsson, P.-E. and Aldén, M., *Appl. Phys. B* 60:51-59 (1995).
  26. Smyth, K. C., Miller, J. H., Dorfman, R. C., Mallard, W. G., and Santoro, R. J., *Combust. Flame* 62:157-181 (1985).
  27. Miller, J. H., Mallard, W. G., and Smyth, K. C., *Combust. Flame* 47:205-214 (1982) and references therein.
  28. Ni, T., Gupta, S. B., and Santoro, R. J., *Twenty-Fifth Symposium (International) on Combustion*, The Combustion Institute, Pittsburgh, 1994, p. 585.
  29. Seitzman, J. M., Hanson, R. K., DeBarber, P. A., and Hess, C. F., *Appl. Opt.* 33:4000-4012 (1994).
  30. Norton, T. S., Smyth, K. C., Miller, J. H., and Smooke, M. D., *Combust. Sci. Technol.* 90:1-34 (1993).
  31. Creitz, E. C., *J. Res. Natl. Bur. Stand.* 65A:389-396 (1961).
  32. VanDerWege, B. A., Bush, M. T., Hochgreh, S., and Linteris, G. T., Technical Meeting of the Eastern States Section of the Combustion Institute, Worcester, MA, 1995, pp. 443-446.
  33. Milne, T. A., Green, C. L., and Benson, D. K., *Combust. Flame* 15:255-264 (1970).
  34. Niioka, T., Mitani, T., and Takahashi, M., *Combust. Flame* 50:89-97 (1983).
  35. Trees, D., Grudno, A., Ilincic, N., Weißweiler, T., and Seshadri, K., Joint Technical Meeting of the Central and Western States (USA) Sections and the Mexican National Section of the Combustion Institute, San Antonio, TX, April, 1995, Paper 95S-045.
  36. Huber, K. P. and Herzberg, G., *Molecular Spectra and Molecular Structure, IV. Constants of Diatomic Molecules*, Van Nostrand Reinhold, New York, 1979.
  37. Tsang, W., personal communication, December, 1995.
  38. Burgess, D. R. F. Jr., Zachariah, M. R., Tsang, W., and Westmoreland, P. R., "Thermochemical and Chemical Kinetic Data for Fluorinated Hydrocarbons," NIST Technical Note 1412, 1995.
  39. Frenklach, M., Clary, D. W., Gardiner, W. C. Jr., and Stein, S. E., *Twenty-First Symposium (International) on Combustion*, The Combustion Institute, Pittsburgh, 1986, p. 1067.

## COMMENTS

Andy Astill, AEA Technology plc, UK. In your talk you posed the question as to why the soot volume fraction went up as the percentage of agent increased. You postulated that this may have a connection with hydrogen levels and

their effect on H-recombination. Could you comment on whether your *observed decrease* in OH might also be a contributory factor given the OH radical's role in soot oxidation. In other words the agent may be causing a reduc-

tion in soot oxidation rather than an increase in soot production.

*Author's Reply.* The processes of soot inception, growth, and oxidation occur sequentially in these co-flowing, axisymmetric flames [1], with oxidation important only in approximately the upper one third of the visible flame. We observe that OH concentrations decrease with increasing agent additions at low heights above the burner, i.e., at early times. Here the OH and soot layers are spatially distinct and OH is not involved in soot oxidation. However, soot production increases significantly with agent addition, despite the fact that H-atom levels are presumably lower than in the uninhibited flame. This then is the puzzle: how can the rates of chemical growth increase while H-atom concentrations are falling? Other species, such as  $\text{CF}_3$ , must be involved in the soot inception chemistry for these inhibited flames.

## REFERENCE

1. Puri, R., Richardson, T. F., Santoro, R. J., and Dobbins, R. A., *Combust. Flame* 92:320-333 (1993).

•

*Van Tiggelen, Lab. Physics Chimie de la Combustion, Belgium.* Is it not before extinguishment that a premixed flame is stabilized on the burner? It seems to appear as a cone in some of your records.

*Author's Reply.* Starting at approximately one half the concentration required for extinction, we do observe stable lifted flames in our co-flowing, axisymmetric conditions. Thus, partial premixing of the propane and air certainly does occur at extinction. However, the "cone" apparent in some of our images for conditions close to extinction (shown in the oral presentation only) is not due to OH alone, but rather we believe arises from an overlap of both OH and PAH fluorescence.